Development and Validation of Velocimeter LIDAR Simulator

Ramchander Bhaskara[1], Roshan Eapen[2], David Van Wijk[1], Davis Adams[3], Caleb Peck[1] and Manoranjan Majji[1]
[1]Texas A&M University, [2]Penn State University, [3]NASA JSC
Correspondence: bhaskara@tamu.edu
AEROSPACE ENGINEERING TEXAS A&M UNIVERSITY
Land Air & Space Robotics Laboratory

Introduction

Motivation

Doppler lidars are capable of providing high-fidelity altimetry and velocimetry, making them versatile instruments in precise navigation and safe landing. Realistic simulation of Doppler lidars and subsequent validation is paramount for their adoption in hardware-in-the-loop simulations for testing flight software and hardware.

Contributions

- NaRPA: A ray-tracing engine for photorealistic imaging and frequency modulated carrier wave (FMCW)/ Doppler/velocimeter lidar emulation.
- Real world and synthetic Doppler lidar datasets with imagery and motion ground truth.
- Performance evaluation of generated synthetic data in comparison to experimental data.

3D assets and motion inference

Mesh and Texture Reconstruction

- Image-based dense 3D reconstruction using COLMAP. Point cloud to mesh (.obj format) using MeshLab.

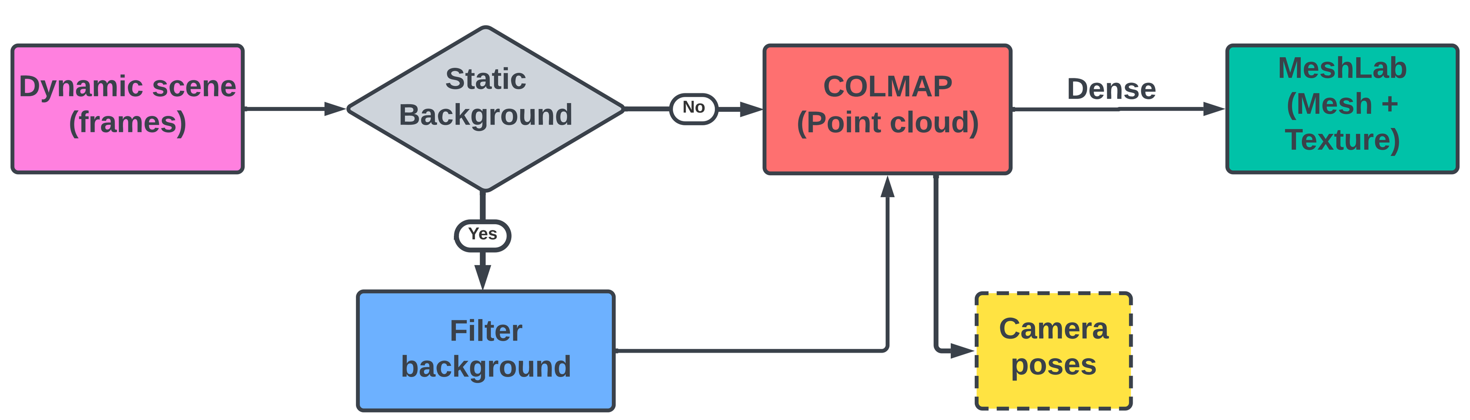

Motion

- Ground truth trajectories using motion capture system (Vicon).
- If motion capture is unavailable: NaRPA metadata is acquired from COLMAP and camera-lidar intrisics.

$$\mathbf{u} = \begin{bmatrix} \mathbf{u}_\theta \\ \mathbf{u}_t \end{bmatrix} \quad \begin{matrix} \text{Rotation} \\ \text{Translation} \end{matrix}$$

$$\boldsymbol{\omega} \approx \frac{\mathbf{u}_\theta}{\Delta t} \qquad \mathbf{v} \approx \frac{\mathbf{u}_t}{\Delta t}$$

Sample interval

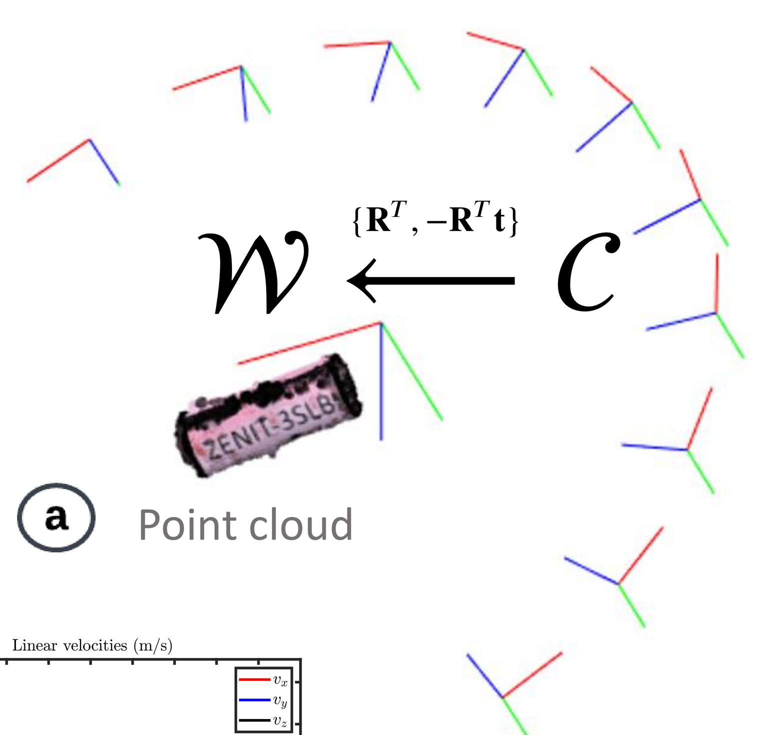

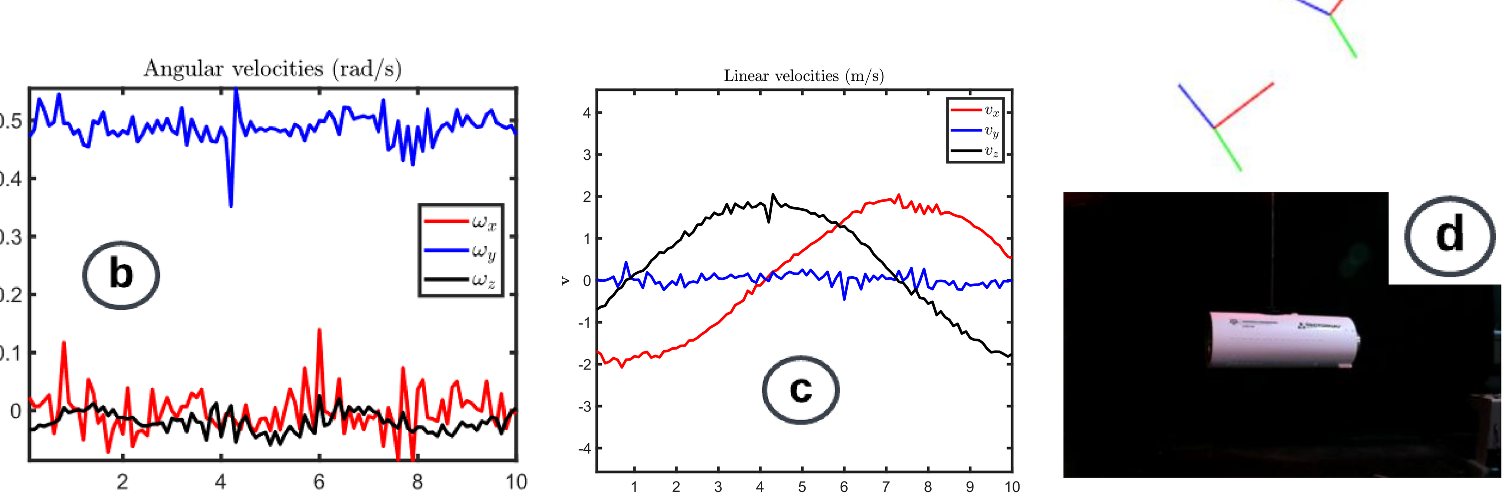

Figure: Camera poses around reconstructed point cloud object in world frame (**a**). Approximate angular and linear velocities from sensor and reconstruction metadata (**b & c**). Frame from our spinning satellite experiment (**d**).

FMCW Lidar Simulation

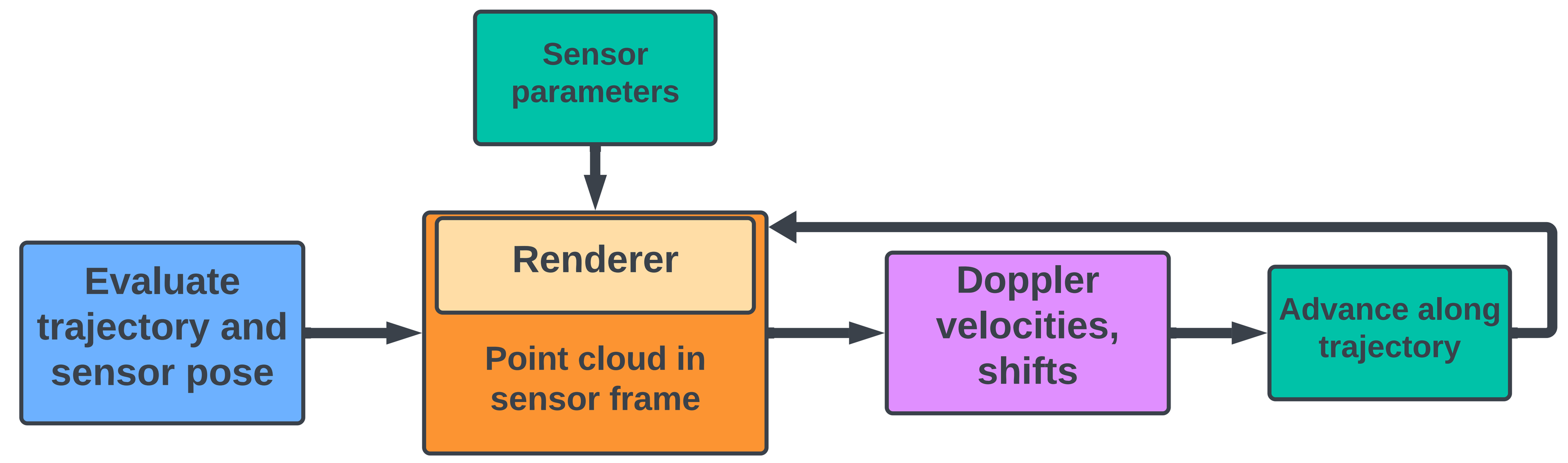

Sensor parameters

Source wavelength, frame rate, sensor orientation, frequency/range rate resolution, spatial resolution, scan rate and noise.

Doppler Velocity Measurement

Instantaneous relative velocity and frequency shift measurement along the lidar's line of sight.

$$v_i = \hat{\mathbf{r}}_i \cdot (-\mathbf{v} + \boldsymbol{\omega} \times \mathbf{t}_s)$$

Doppler velocity (v_i), Measurement direction ($\hat{\mathbf{r}}_i$), Sensor Velocity ($\mathbf{v}$), Angular Velocity ($\boldsymbol{\omega}$), Sensor Translation ($\mathbf{t}_s$)

$$\Delta f = \frac{2v_i}{\lambda}$$

Doppler shift (Δf), Doppler velocity (v_i), Lidar Wavelength (λ)

Rendering System Setup

Trajectory information from motion capture system to setup object and sensor in the world frame of NaRPA (renderer). NaRPA follows openGL convention.

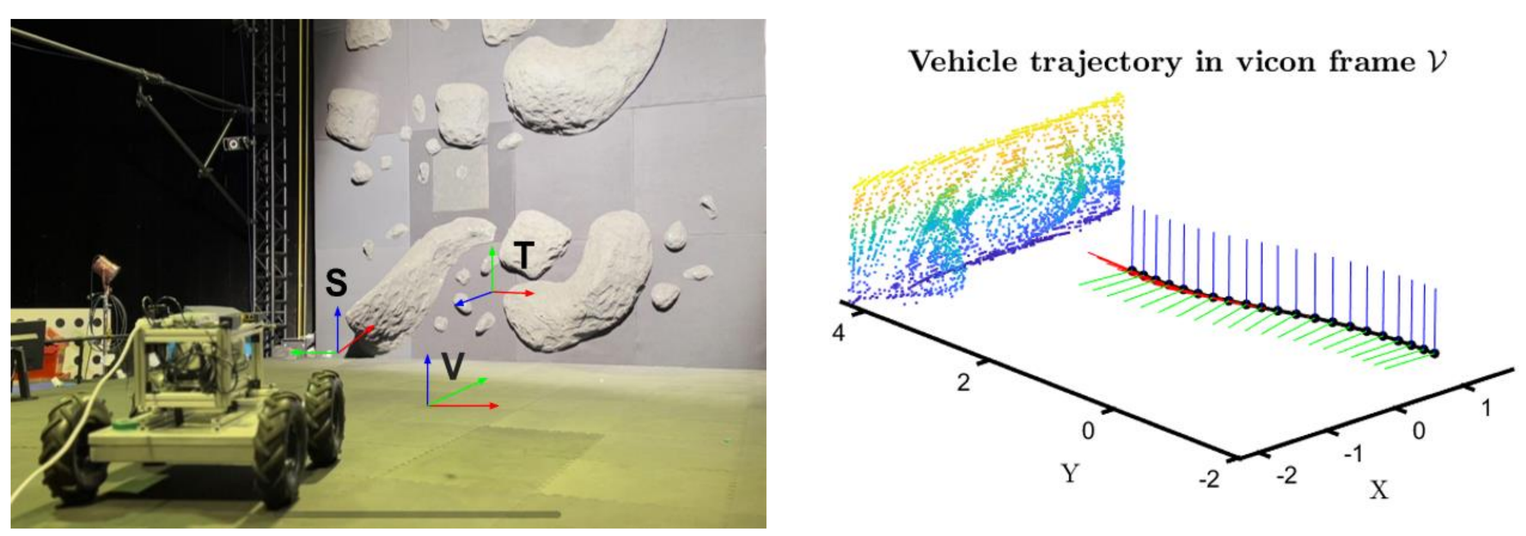

Figure: Asteroid wall data collection campaign at JPL (left). Reconstructed point cloud and ground truth trajectory from vicon (right).

EDL Applications

Targeted towards entry, descent, and landing (EDL) sensor simulation, NaRPA is used for dataset generation in studies including terrain relative navigation, proximity operations, and differentiable rendering.

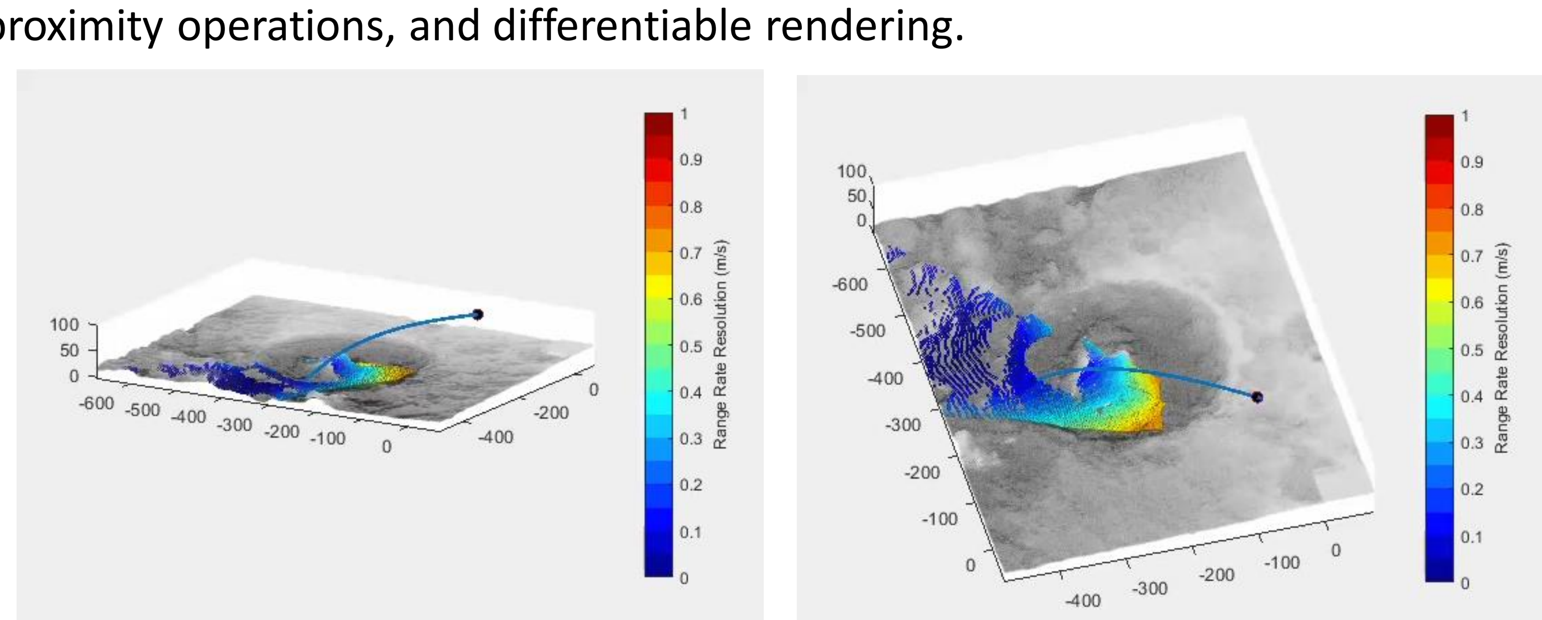

Validation

Result: Doppler velocities visualization

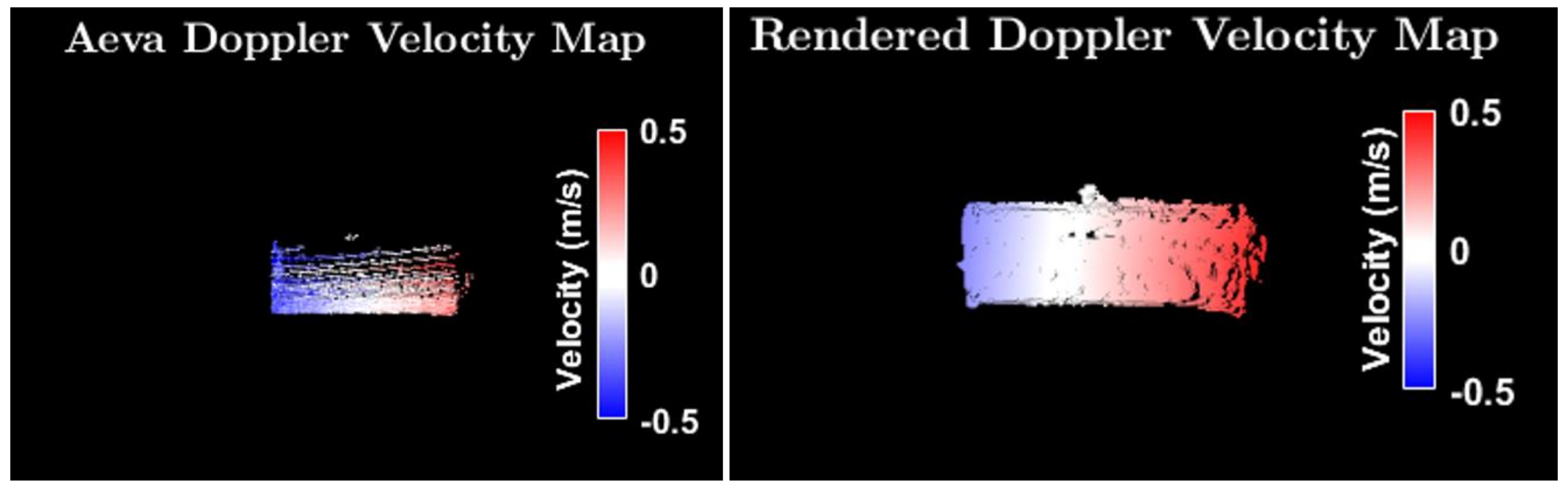

Figure:Point cloud and instant velocities from Aeva lidar (left). Reconstructed point cloud and velocities evaluated at corresponding frame (right).

Result: Doppler velocity distributions

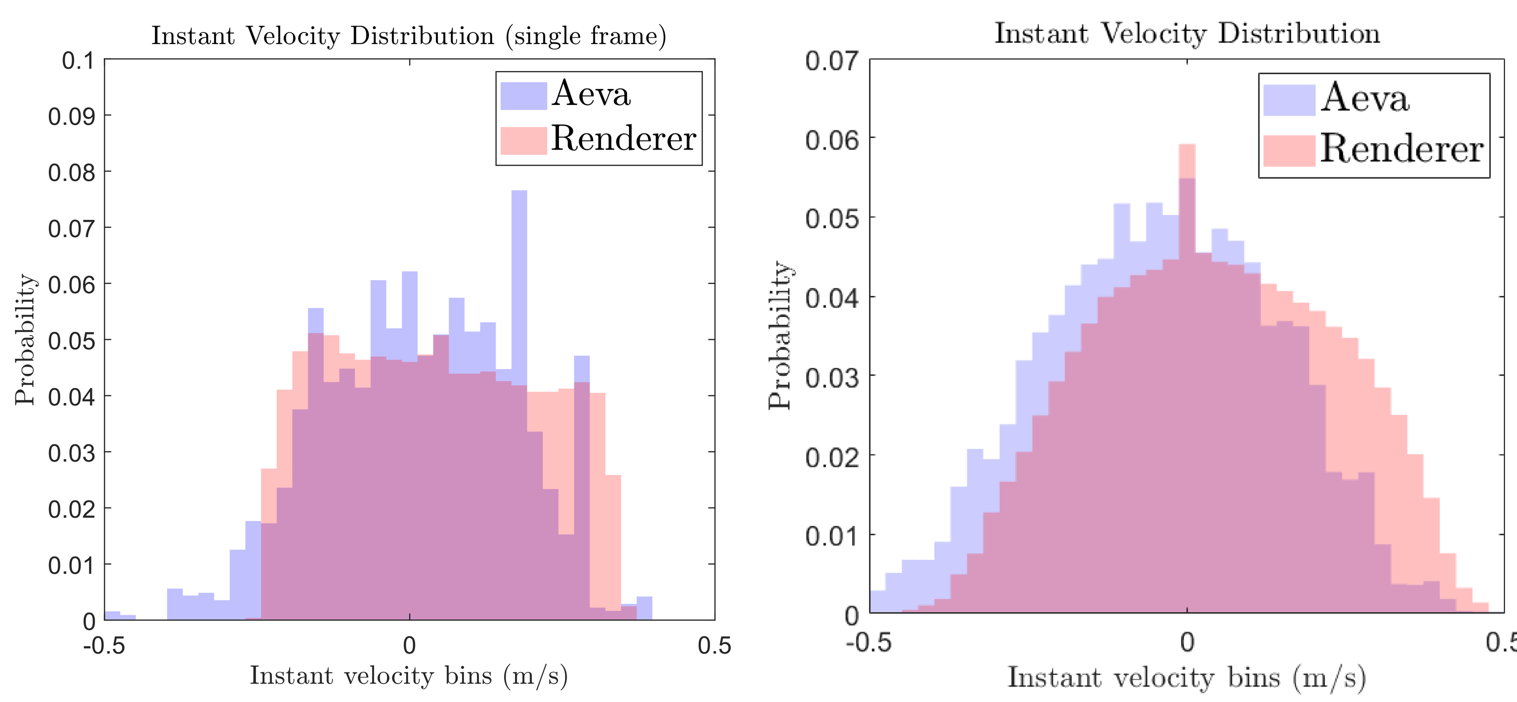

Figure: Normalized histograms of Doppler velocities as a metric to quantify the distribution of instantaneous point velocities. Aeva velocities and corresponding rendered point cloud velocities for a chosen single frame (left), and averaged velocities across 100 frames (right).

Median Absolute Deviation

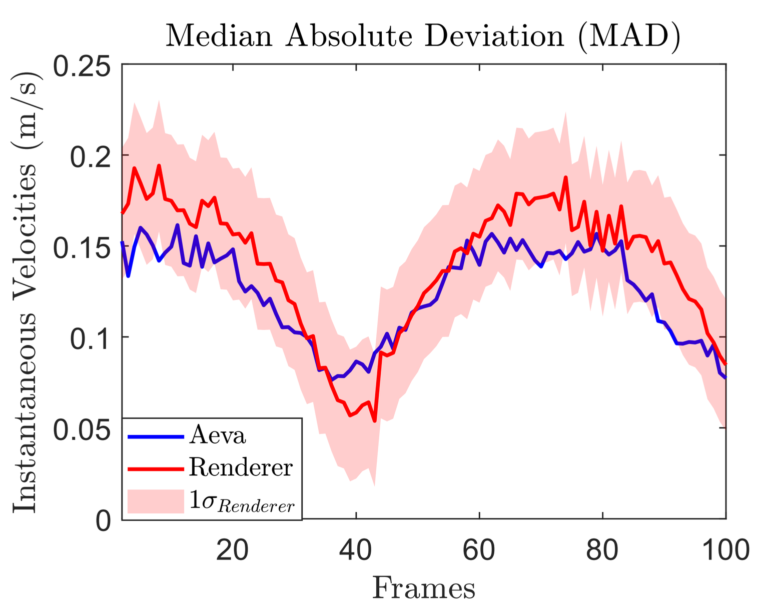

Figure: Median Absolute Deviations (MAD) of point velocities from NaRPA (red) and Aeva (blue). Renderer following the velocity distribution of the sensor within 1-sigma bounds.

Point Cloud Sample Variance

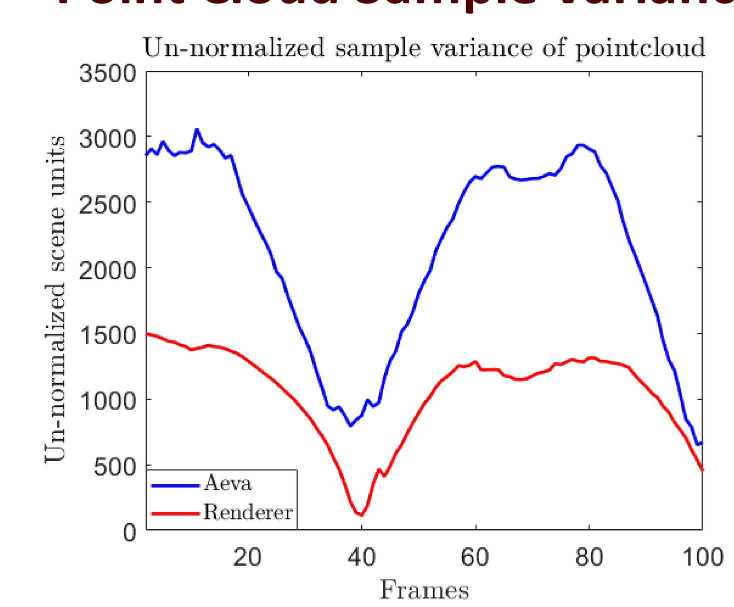

Figure: Un-normalized variances of point clouds of rendered points (red) and Aeva points (blue). Matching shapes indicate similarity in point cloud "spreadedness" across frames.

Acknowledgements

JPL: Sarah Stevens, Anup Katake, Tejas Kulkarni, Alejandro San Martin, Nicolas Trawney, Eli Skulsky., Carolina Restrepo (NASA-GSFC), Ronney Lovelace (JSC)., Daniel Crispell (VSI), Joe Mundy (VSI)., Jerry Tessendorf (Clemson).